Elastostatics of Nonuniform Miniaturized Beams: Explicit Solutions Through a Nonlocal Transfer Matrix Formulation *+

Hossein Darban[1]

Institute of Fundamental Technological Research, Polish Academy of Sciences, Pawińskiego 5B, 02-106 Warsaw, Poland

[1]- ***Corresponding author:*** *Hossein Darban*; ***E-mail addresses:*** *hdarban@ippt.pan.pl*; ***Tel.:*** *(+48) 22 826 12 81*

+Published in the International Journal of Engineering Science, Volume 198, 1 May 2024, 104054.
doi: 10.1016/j.ijengsci.2024.104054

Abstract

A mathematically well-posed nonlocal model is formulated based on the variational approach and the transfer matrix method to investigate the elastostatics of nonuniform miniaturized beams. These beams are composed of an arbitrary number of sub-beams with diverse material and geometrical properties, as well as small-scale size dependency. The model adopts a stress-driven nonlocal approach, a well-established framework in the Engineering Science community. The curvature of a sub-beam is defined through an integral convolution, considering the bending moments across all cross-sections of the sub-beam and a kernel function. The governing equations are solved and the deflections are derived in terms of some constants. The formulation employs local and interfacial transfer matrices, incorporating continuity conditions at cross-sections where sub-beams are joined, to define relations between constants in the solution of a generic sub-beam and those of the first sub-beam at the left end. The boundary conditions are then imposed to derive an explicit, closed-form solution for the deflection. This solution significantly facilitates the study of nonuniform beams with many sub-beams. The study explores nonuniform beams made of two to five different sub-beams. The results are presented with an emphasis on the effects of the material properties, nonlocalities, and lengths of the sub-beams on the deflection. The results reveal the intricate behavior of nonlocal nonuniform beams, showcasing complexity in contrast to the predictable responses observed in the bending of the local nonuniform beams.

Keywords: Small-scale beam; Transfer matrix method; Multi-material; Size effect; MEMS and NEMS.

1. Introduction

1.1. Miniaturized Structures and Modeling Strategies

The advent of small-scale structures has revolutionized several technological domains in the Engineering Science community by introducing significant improvements in the functionality of smart devices and systems. These structures with micro- and nanoscale dimensions have become integral components in the construction of devices in many fields ranging from electronics and optics to medicine and materials science [1–4]. For instance, micro- and nanostructures, including nanobeams, nanotubes, nanoplates, and nanoshells, find extensive applications, contributing to advancements in energy harvesters, fluid conveying devices, nanoswitches, nanoactuators, nanosensors, and nanoresonators. The unique mechanical properties of these intelligent miniaturized structures open new avenues for innovation.

Recent advancements have introduced novel types of micro- and nanostructures, including those constructed from functionally graded [5–7] or porous [8–10] materials, having sandwich configurations [11, 12], or composed of multiple layers [13, 14].

Along with the progress in technology and beyond the atomistic models [15, 16], pioneering nonclassical continuum mechanics-based theories have emerged within the community of Engineering Science, able to model the mechanical response of small-scale structures accurately. The commonly employed theories include the couple stress theory [17], strain gradient theory [18], micropolar theory [19], nonlocal elasticity [20], surface elasticity theory [21], theories based on fractional calculus [22], modified couple stress theory [23], modified strain gradient theory [24], and nonlocal strain gradient theory [25]. These theories have been used extensively to study the mechanical behavior of small-scale structures [26–43]. The new generations of miniaturized structures present unique challenges and opportunities, demanding more efficient and innovative models for their comprehensive study and understanding. For instance, the phase field method and surface elasticity theory are combined in [34] to develop a powerful tool for studying the fracture mechanics of ultra-thin films at micro- and nanoscale. Another example is in [13], where three-dimensional thermoelastic solutions are derived for nonlocal multilayered plates with imperfect interfaces using matrix techniques. In [44], a nonlocal layerwise formulation is developed for the bending of multilayered miniaturized beams featuring weak bonding.

1.2. Nonuniform Miniaturized Beam

The term " nonuniform miniaturized beam" in this paper refers to a small-scale beam element composed of different sub-beams along its length. These sub-beams may be made of various materials and possess different geometries and small-scale size dependencies. The primary objective of creating a nonuniform miniaturized beam is often to tailor its overall properties, such as flexibility or strength. This engineering approach enables the optimization of the performance of the miniaturized beams for specific applications or under particular loading conditions. For instance, having control over the deflection profile of a small-scale beam can be crucial for optimizing design, enabling sensing and actuation functionalities, and ensuring the reliable operation of small-scale devices across various applications. Two notable examples of nonuniform miniaturized beams include (i) a micro- or nanomechanical cantilever mass sensor with a wider cross-section near the free end, as depicted in Fig. 1(a), and (ii) a micro- or nanomechanical fixed-fixed mass sensor with a wider cross-section at the midspan, as shown in Fig. 1(b). These specific geometries are often designed to increase the likelihood of binding entities such as viruses near the tip or midspan of the sensor to maximize the effect of added mass. The nonuniform miniaturized beams belong to the category of innovative small-scale beams, and studying their mechanical response is essential.

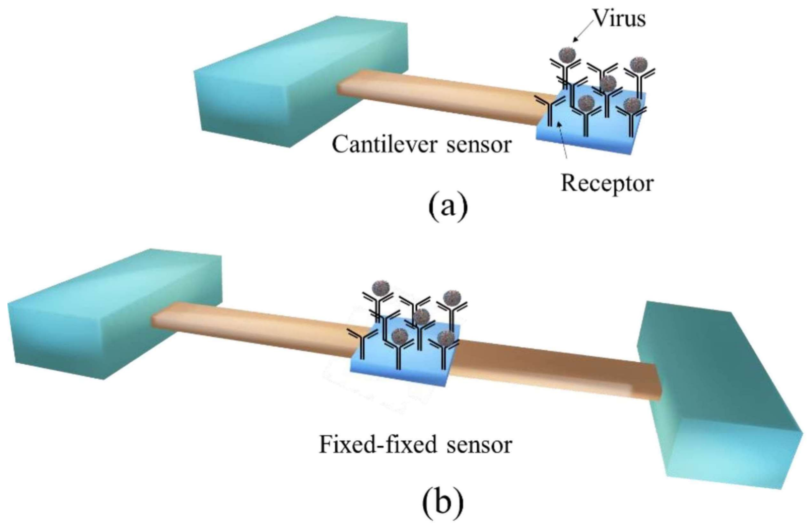

Fig. 1 Miniaturized (a) cantilever and (b) fixed-fixed mass sensors.

1.3. Objective

In this paper, the flexural response of a nonuniform miniaturized beam, composed of any arbitrary number of sub-beams, is studied. The experimentally observed size effect in small-scale structures [45, 46] is incorporated into the formulation by using a stress-driven type of nonlocal elasticity [47]. In this manner, the curvature of a cross-section within a sub-beam is defined by an integral convolution expressed in terms of all the bending moments across that sub-beam and a kernel function. The integral form of the nonlocal constitutive equation is first converted to a differential form and then used to express the Bernoulli-Euler equilibrium equations of each sub-beam in terms of deflection. The equilibrium equation is solved in a closed-form, and the solution is derived in terms of some unknown constants. The transfer matrix method, originally presented by Thomson in [48] and later corrected by Haskel in [49] for addressing the propagation of plane elastic waves in a layered medium submerged in a fluid, is used to derive the unknown constants and present an explicit closed-form solution for the deflection of the nonuniform miniaturized beam with any arbitrary number of sub-beams.

The article is structured as described in the following. The problem definition and the nonlocal formulation are presented in Sect. 2. The closed-form solution is derived in Sect. 3 through the application of the transfer matrix method. The obtained closed-form solution is used in Sect. 4 to investigate the bending of nonuniform miniaturized beams with two to five sub-beams. The conclusions of the work are presented in Sect. 5.

2. Problem Definition and Nonlocal Formulation

As shown in Fig. 2, a general case of a small-scale beam composed of n different homogeneous and isotropic sub-beams under flexural deformations is considered. The sub-beams, numbered from left to right, may have varying material properties and cross-sections. They are perfectly connected end-to-end at locations x_i for i = 1, …, n-1, with the shown coordinate system. Without loss of generality, we consider that the small-scale beam is subjected to a uniform distributed load denoted by q. The flexural response of the beam under any other loading distributions can be studied similarly.

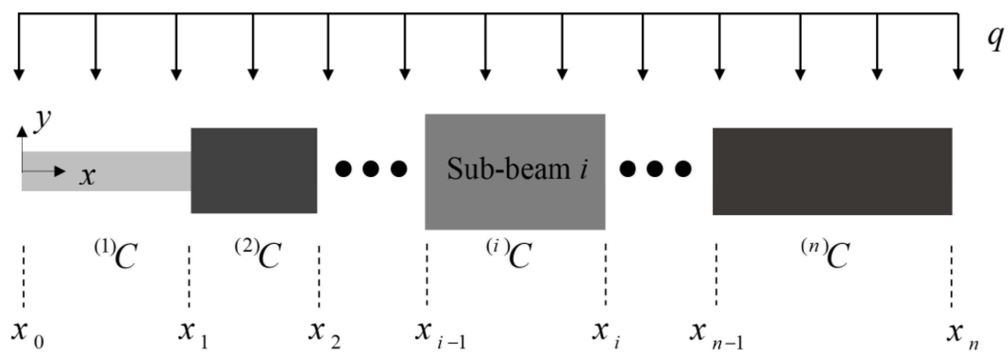

Fig. 2 Small-scale beam made of n different sub-beams subjected to a uniform distributed load.

Based on the stress-driven theory of nonlocal elasticity [47], the curvature of a generic sub-beam i, ${}^{(i)}\chi$, is related to the bending moment distribution along the length of the sub-beam, ${}^{(i)}M$, as:

$$ {}^{(i)}\chi\left(x\right)=\int_{x_{i-1}}^{x_i}\frac{0.5}{{}^{(i)}L_C}e^{\left(-\frac{|x-\xi|}{{}^{(i)}L_C}\right)}\,{}^{(i)}C\,{}^{(i)}M\left(\xi\right)d\xi \tag{1} $$

for i = 1, …, n. Here and throughout the derivation, ${}^{(i)}F$ indicates the quantity F defined across the sub-beam i. The elastic compliance of the sub-beam is ${}^{(i)}C={}^{(i)}\left(EI\right)^{-1}$, with ${}^{(i)}E$ Young's modulus and ${}^{(i)}I$ the second moment of area of the sub-beam. The kernel function is $0.5e^{\left(-|x-\xi|/{}^{(i)}L_C\right)}\Big/{}^{(i)}L_C$. The length scale parameter, ${}^{(i)}L_C$, controls the intensity of nonlocality of the sub-beam i, such that when the length scale parameter approaches zero, the local formulation is restored.

The constitutive behavior of sub-beam i, presented in Eq. (1), is not affected by the bending distributions of other sub-beams since the integration is defined only across sub-beam i. Therefore, the equation is valid under the assumption that the nonlocalities of the sub-beams are independent. This assumption aligns with the fact that the small-scale beam is formed by connecting individual, distinct sub-beams. Although there may exist some subtle interactions between the nonlocality of sub-beams due to the continuity of displacements and stresses at the cross-sections where the sub-beams are connected, these effects are disregarded for the sake of simplicity. In addition, this assumption allows for the derivation of explicit closed-form solutions of the problem, as presented in Sect. 3.

Following the standard manipulation in nonlocal beam theories, decomposing the constitutive relation in Eq. (1) for $x_{i-1} \le \xi \le x$ and $x \le \xi \le x_i$, and taking two derivatives of the relation, the integral nonlocal constitutive relation given in Eq. (1) is reformulated as the following differential equation:

$$ {}^{(i)}\chi - {}^{(i)}L_C^2 \, {}^{(i)}\chi_{,xx} = {}^{(i)}C \, {}^{(i)}M \tag{2} $$

with the associated constitutive boundary conditions:

$$ \begin{aligned} {}^{(i)}\chi_{,x}\left(x_{i-1}\right) &= \frac{1}{{}^{(i)}L_C} \, {}^{(i)}\chi\left(x_{i-1}\right) \\ {}^{(i)}\chi_{,x}\left(x_{i}\right) &= -\frac{1}{{}^{(i)}L_C} \, {}^{(i)}\chi\left(x_{i}\right) \end{aligned} \tag{3} $$

for $i = 1, \ldots, n$. Here and throughout the derivation, $F_{\underbrace{,xxx\ldots x}_{j\text{ times}}} = \frac{d^j F}{dx^j}$.

Considering the bending equation of the Bernoulli-Euler beam, $M_{,xx}\left(x\right) + q = 0$, Eq.(2), and the curvature-deflection relation, ${}^{(i)}\chi = {}^{(i)}v_{,xx}$, the equation governing the flexural response of sub-beam i reads:

$$ {}^{(i)}L_C^2 \, {}^{(i)}v_{,xxxxxx} - {}^{(i)}v_{,xxxx} - {}^{(i)}Cq = 0 \tag{4} $$

for $i = 1, \ldots, n$. The solution of the sixth-order ordinary differential equation (4) for sub-beam i involves six unknown constants which make the solution of the entire beam to depend on $6 \times n$ unknown constants. The constants are determined by imposing the following $4 \times \left(n-1\right)$ variationally consistent continuity conditions at the cross-sections where the sub-beams are connected:

$$
\begin{aligned}
&{}^{(i+1)}v\left(x_i\right)={}^{(i)}v\left(x_i\right)\\
&{}^{(i+1)}v_{,x}\left(x_i\right)={}^{(i)}v_{,x}\left(x_i\right)\\
&\frac{{}^{(i+1)}v_{,xx}\left(x_i\right)-{}^{(i+1)}L_C^2\,{}^{(i)}v_{,xxxx}\left(x_i\right)}{{}^{(i+1)}C}=\frac{{}^{(i)}v_{,xx}\left(x_i\right)-{}^{(i)}L_C^2\,{}^{(i)}v_{,xxxx}\left(x_i\right)}{{}^{(i)}C}\\
&\frac{{}^{(i+1)}v_{,xxx}\left(x_i\right)-{}^{(i+1)}L_C^2\,{}^{(i)}v_{,xxxxx}\left(x_i\right)}{{}^{(i+1)}C}=\frac{{}^{(i)}v_{,xxx}\left(x_i\right)-{}^{(i)}L_C^2\,{}^{(i)}v_{,xxxxx}\left(x_i\right)}{{}^{(i)}C}
\end{aligned}
\tag{5}
$$

for $i = 1, \ldots, n\text{-}1$. The first two equations satisfy the kinematic continuity conditions, while the last two equations ensure the continuity of bending moment and shear force at the cross-sections where the sub-beams are connected. The remaining equations are $2\times n$ constitutive boundary conditions (3) at the sub-beam ends, which in terms of the sub-beam deflections are expressed as:

$$
\begin{aligned}
&{}^{(i)}v_{,xxx}\left(x_{i-1}\right)=\frac{1}{{}^{(i)}L_C}\,{}^{(i)}v_{,xx}\left(x_{i-1}\right)\\
&{}^{(i)}v_{,xxx}\left(x_i\right)=-\frac{1}{{}^{(i)}L_C}\,{}^{(i)}v_{,xx}\left(x_i\right)
\end{aligned}
\tag{6}
$$

and four boundary conditions at the beam's ends, x_0 and x_n:

$$
\text{Fixed-Free}\begin{cases}{}^{(1)}v(0)=0\\ {}^{(1)}v_{,x}(0)=0\\ {}^{(n)}v_{,xx}(L)-{}^{(n)}L_C^2\,{}^{(n)}v_{,xxxx}(L)=0\\ {}^{(n)}v_{,xxx}(L)-{}^{(n)}L_C^2\,{}^{(n)}v_{,xxxxx}(L)=0\end{cases};\quad
\text{Fixed-Fixed}\begin{cases}{}^{(1)}v(0)=0\\ {}^{(1)}v_{,x}(0)=0\\ {}^{(n)}v(L)=0\\ {}^{(n)}v_{,x}(L)=0\end{cases}
$$

$$
\text{Pinned-Pinned}\begin{cases}{}^{(1)}v(0)=0\\ {}^{(1)}v_{,xx}(0)-{}^{(1)}L_C^2\,{}^{(1)}v_{,xxxx}(0)=0\\ {}^{(n)}v(L)=0\\ {}^{(n)}v_{,xx}(L)-{}^{(n)}L_C^2\,{}^{(n)}v_{,xxxx}(L)=0\end{cases};\quad
\text{Fixed-Pinned}\begin{cases}{}^{(1)}v(0)=0\\ {}^{(1)}v_{,x}(0)=0\\ {}^{(n)}v(L)=0\\ {}^{(n)}v_{,xx}(L)-{}^{(n)}L_C^2\,{}^{(n)}v_{,xxxx}(L)=0\end{cases}
\tag{7}
$$

To facilitate the presentation of the numerical results, Eqs. (4)-(7) are normalized as:

$$
{}^{(i)}\lambda^2\,{}^{(i)}\bar{v}_{,\overline{xxxxxx}}-{}^{(i)}\bar{v}_{,\overline{xxxx}}-{}^{(i)}\bar{C}=0, \tag{8}
$$

$$
\begin{aligned}
&{}^{(i+1)}\bar{v}\left(\bar{x}_i\right) = {}^{(i)}\bar{v}\left(\bar{x}_i\right)\\
&{}^{(i+1)}\bar{v}_{,x}\left(\bar{x}_i\right) = {}^{(i)}\bar{v}_{,x}\left(\bar{x}_i\right)\\
&\frac{{}^{(i+1)}\bar{v}_{,\overline{xx}}\left(\bar{x}_i\right) - {}^{(i+1)}\lambda^2\,{}^{(i)}\bar{v}_{,\overline{xxxx}}\left(\bar{x}_i\right)}{{}^{(i+1)}\bar{C}} = \frac{{}^{(i)}\bar{v}_{,\overline{xx}}\left(\bar{x}_i\right) - {}^{(i)}\lambda^2\,{}^{(i)}\bar{v}_{,\overline{xxxx}}\left(\bar{x}_i\right)}{{}^{(i)}\bar{C}} \quad ,\\
&\frac{{}^{(i+1)}\bar{v}_{,\overline{xxx}}\left(\bar{x}_i\right) - {}^{(i+1)}\lambda^2\,{}^{(i)}\bar{v}_{,\overline{xxxxx}}\left(\bar{x}_i\right)}{{}^{(i+1)}\bar{C}} = \frac{{}^{(i)}\bar{v}_{,\overline{xxx}}\left(\bar{x}_i\right) - {}^{(i)}\lambda^2\,{}^{(i)}\bar{v}_{,\overline{xxxxx}}\left(\bar{x}_i\right)}{{}^{(i)}\bar{C}}
\end{aligned}
\tag{9}
$$

$$
\begin{aligned}
&{}^{(i)}\bar{v}_{,\overline{xxx}}\left(\bar{x}_{i-1}\right) = \frac{1}{{}^{(i)}\lambda}\,{}^{(i)}\bar{v}_{,\overline{xx}}\left(\bar{x}_{i-1}\right)\\
&{}^{(i)}\bar{v}_{,\overline{xxx}}\left(\bar{x}_i\right) = -\frac{1}{{}^{(i)}\lambda}\,{}^{(i)}\bar{v}_{,\overline{xx}}\left(\bar{x}_i\right)
\end{aligned}
\tag{10}
$$

and,

$$
\text{Fixed-Free}\begin{cases}
{}^{(1)}\bar{v}(0)=0\\
{}^{(1)}\bar{v}_{,\bar{x}}(0)=0\\
{}^{(n)}\bar{v}_{,\overline{xx}}(1)-{}^{(n)}\lambda^2\,{}^{(n)}\bar{v}_{,\overline{xxxx}}(1)=0\\
{}^{(n)}\bar{v}_{,\overline{xxx}}(1)-{}^{(n)}\lambda^2\,{}^{(n)}\bar{v}_{,\overline{xxxxx}}(1)=0
\end{cases};\quad
\text{Fixed-Fixed}\begin{cases}
{}^{(1)}\bar{v}(0)=0\\
{}^{(1)}\bar{v}_{,\bar{x}}(0)=0\\
{}^{(n)}\bar{v}(1)=0\\
{}^{(n)}\bar{v}_{,\bar{x}}(1)=0
\end{cases}
$$

$$
\text{Pinned-Pinned}\begin{cases}
{}^{(1)}\bar{v}(0)=0\\
{}^{(1)}\bar{v}_{,\overline{xx}}(0)-{}^{(1)}\lambda^2\,{}^{(1)}\bar{v}_{,\overline{xxxx}}(0)=0\\
{}^{(n)}\bar{v}(1)=0\\
{}^{(n)}\bar{v}_{,\overline{xx}}(1)-{}^{(n)}\lambda^2\,{}^{(n)}\bar{v}_{,\overline{xxxx}}(1)=0
\end{cases};\quad
\text{Fixed-Pinned}\begin{cases}
{}^{(1)}\bar{v}(0)=0\\
{}^{(1)}\bar{v}_{,\bar{x}}(0)=0\\
{}^{(n)}\bar{v}(1)=0\\
{}^{(n)}\bar{v}_{,\overline{xx}}(1)-{}^{(n)}\lambda^2\,{}^{(n)}\bar{v}_{,\overline{xxxx}}(1)=0
\end{cases}
\tag{11}
$$

The dimensionless parameters in Eqs. (8)-(11) are:

$$
\bar{x}=\frac{x}{L};\quad {}^{(i)}\bar{v}=\frac{{}^{(i)}v}{q\,{}^{(1)}CL^4};\quad {}^{(i)}\bar{C}=\frac{{}^{(i)}C}{{}^{(1)}C};\quad {}^{(i)}\lambda=\frac{{}^{(i)}L_C}{L},
\tag{12}
$$

3. Closed-Form Solutions Through the Transfer Matrix Method

The closed-form solution of the governing equation (8) is given by:

$$
{}^{(i)}\bar{v}={}^{(i)}A_1\bar{x}^3+{}^{(i)}A_2\bar{x}^2+{}^{(i)}A_3\bar{x}+{}^{(i)}A_4+{}^{(i)}A_5\,{}^{(i)}\lambda^4 e^{x/{}^{(i)}\lambda}+{}^{(i)}A_6\,{}^{(i)}\lambda^4 e^{-x/{}^{(i)}\lambda}-{}^{(i)}\bar{C}\,\bar{x}^4/24
\tag{13}
$$

where ${}^{(i)}A_j$ for j = 1, …, 6 are the unknown constants related to the sub-beam *i.* The imposition of the two constitutive boundary conditions at the ends of the sub-beams, as given in Eq. (10), allows the derivation of the constants ${}^{(i)}A_5$ and ${}^{(i)}A_6$. This leads to the simplification of the solution presented in Eq. (13) to the following form in terms of only four unknown constants ${}^{(i)}A_j$ for $j = 1, \ldots, 4$:

$$
\begin{aligned}
{}^{(i)}\bar{v} = {}& {}^{(i)}A_1\bar{x}^3 + {}^{(i)}A_2\bar{x}^2 + {}^{(i)}A_3\bar{x} + {}^{(i)}A_4 - {}^{(i)}\bar{C}\,\bar{x}^4/24 + \\
&+ \frac{2\,{}^{(i)}\bar{C}\,\bar{x}_i\,{}^{(i)}\lambda + {}^{(i)}\bar{C}\,\bar{x}_i^2 - 12\,{}^{(i)}A_1\,{}^{(i)}\lambda - 12\,{}^{(i)}A_1\bar{x}_i - 4\,{}^{(i)}A_2}{4e^{\bar{x}_i/{}^{(i)}\lambda}}\,{}^{(i)}\lambda^2 e^{x/{}^{(i)}\lambda} - \\
&- \frac{2\,{}^{(i)}\bar{C}\,\bar{x}_{i-1}\,{}^{(i)}\lambda - {}^{(i)}\bar{C}\,\bar{x}_{i-1}^2 - 12\,{}^{(i)}A_1\,{}^{(i)}\lambda + 12\,{}^{(i)}A_1\bar{x}_{i-1} + 4\,{}^{(i)}A_2}{4e^{-\bar{x}_{i-1}/{}^{(i)}\lambda}}\,{}^{(i)}\lambda^2 e^{-x/{}^{(i)}\lambda}
\end{aligned}
\tag{14}
$$

The remaining $4\times n$ unknown constants ${}^{(i)}A_j$ for $i = 1, \ldots, n$, and $j = 1, \ldots, 4$ can be derived by imposing continuity conditions in Eq. (9) and boundary conditions in Eq. (11). In the next sections, the transfer matrix method is employed to derive closed-form solution of the displacement.

3.1. Transfer Matrix Method

The general idea of the transfer matrix method is shown in Fig. 3. The procedure consists of two steps. First, the four unknown constants of each sub-beam are derived in terms of the unknown constants of the first sub-beam using local and interfacial transfer matrices. This approach effectively simplifies the problem to finding only the four unknown constants of the first sub-beam. The second step involves defining these four unknown constants by imposing the appropriate boundary conditions.

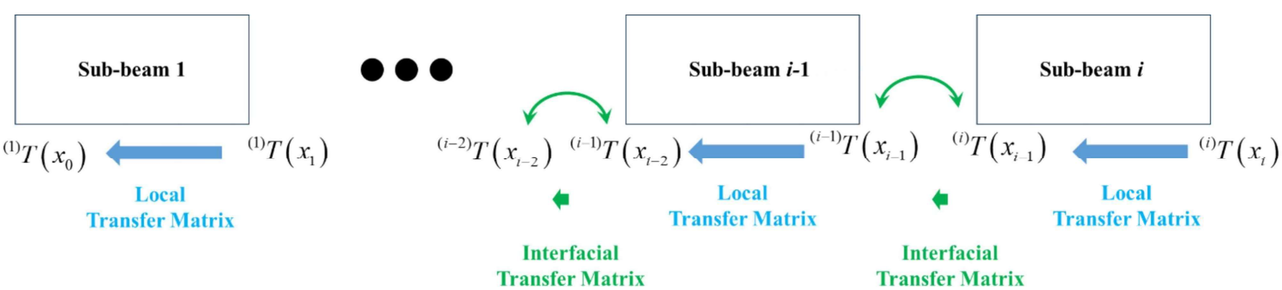

Fig. 3 A schematic description of the transfer matrix method.

To establish a relation between the unknown constants of the generic sub-beam i and those of the first sub-beam, the vector T is introduced in the following way:

$$
{}^{(i)}T(\bar{x}) = {}^{(i)}\begin{bmatrix} \bar{v}(\bar{x}) \\ \bar{v}_{,x}(\bar{x}) \\ \dfrac{\bar{v}_{,\overline{xx}}(\bar{x}) - \lambda^2 \bar{v}_{,\overline{xxxx}}(\bar{x})}{\bar{C}} \\ \dfrac{\bar{v}_{,\overline{xxx}}(\bar{x}) - \lambda^2 \bar{v}_{,\overline{xxxxx}}(\bar{x})}{\bar{C}} \end{bmatrix} \tag{15}
$$

Using the closed-form solution in Eq. (14), the vector T is decomposed as:

$$
{}^{(i)}T(\bar{x}) = {}^{(i)}B(\bar{x}) \; {}^{(i)}\begin{bmatrix} A_1 \\ A_2 \\ A_3 \\ A_4 \end{bmatrix} + {}^{(i)}P(\bar{x}) \tag{16}
$$

where B is a 4×4 matrix given as:

$$
{}^{(i)}B(\bar{x}) = {}^{(i)}\begin{bmatrix} 3\lambda^2(\lambda - \bar{x}_{i-1})e^{(\bar{x}_{i-1}-\bar{x})/\lambda} - 3\lambda^2(\lambda + \bar{x}_i)e^{(-\bar{x}_i+\bar{x})/\lambda} + \bar{x}^3 & -\lambda^2 e^{(\bar{x}_{i-1}-\bar{x})/\lambda} - \lambda^2 e^{(-\bar{x}_i+\bar{x})/\lambda} + \bar{x}^2 & \bar{x} & 1 \\ -3\lambda(\lambda - \bar{x}_{i-1})e^{(\bar{x}_{i-1}-\bar{x})/\lambda} - 3\lambda(\lambda + \bar{x}_i)e^{(-\bar{x}_i+\bar{x})/\lambda} + 3\bar{x}^2 & \lambda e^{(\bar{x}_{i-1}-\bar{x})/\lambda} - \lambda e^{(-\bar{x}_i+\bar{x})/\lambda} + 2\bar{x} & 1 & 0 \\ 6\bar{x}/\bar{C} & 2/\bar{C} & 0 & 0 \\ 6/\bar{C} & 0 & 0 & 0 \end{bmatrix} \tag{17}
$$

and vector P is:

$$
{}^{(i)}P(\bar{x}) = {}^{(i)}\begin{bmatrix} -\dfrac{\left(\left(12\lambda^3 - 6\lambda^2\,\bar{x}_{i-1}\right)\bar{x}_{i-1}e^{(\bar{x}_{i-1}-\bar{x})/\lambda} - \left(12\lambda^3 + 6\lambda^2\,\bar{x}_i\right)\bar{x}_i e^{(-\bar{x}_i+\bar{x})/\lambda} + \bar{x}^4\right)\bar{C}}{24} \\ -\dfrac{\left(-3\lambda\left(\lambda - \bar{x}_{i-1}/2\right)\bar{x}_{i-1}e^{(\bar{x}_{i-1}-\bar{x})/\lambda} - 3\lambda\left(\lambda + \bar{x}_i/2\right)\bar{x}_i e^{(-\bar{x}_i+\bar{x})/\lambda} + \bar{x}^3\right)\bar{C}}{6} \\ -\bar{x}^2/2 + \lambda^2 \\ -\bar{x} \end{bmatrix} \tag{18}
$$

The vector of unknowns of sub-beam i can be defined using Eq. (16):

$$
{}^{(i)}\begin{bmatrix} A_1 \\ A_2 \\ A_3 \\ A_4 \end{bmatrix} = {}^{(i)}B^{-1}\left(\overline{x}\right)\left[{}^{(i)}T\left(\overline{x}\right) - {}^{(i)}P\left(\overline{x}\right)\right] \tag{19}
$$

Note that ${}^{(i)}B^{-1}$ is the inverse of the matrix ${}^{(i)}B$ with $\det\left[{}^{(i)}B\right] \neq 0$. The relationship presented above defines the unknown constants of the generic sub-beam i at any location within the interval $\overline{x}_{i-1} \leq \overline{x} \leq \overline{x}_i$. In particular, if we assume $\overline{x} = \overline{x}_{i-1}$, the vector of unknowns becomes:

$$
{}^{(i)}\begin{bmatrix} A_1 \\ A_2 \\ A_3 \\ A_4 \end{bmatrix} = {}^{(i)}B^{-1}\left(\overline{x}_{i-1}\right)\left[{}^{(i)}T\left(\overline{x}_{i-1}\right) - {}^{(i)}P\left(\overline{x}_{i-1}\right)\right] \tag{20}
$$

The local transfer matrix of sub-beam i which relates ${}^{(i)}T\left(\overline{x}_i\right)$ and ${}^{(i)}T\left(\overline{x}_{i-1}\right)$, can be derived by substituting the unknown vector given in Eq. (20) into Eq. (16) and setting $\overline{x} = \overline{x}_i$:

$$
{}^{(i)}T\left(\overline{x}_i\right) = {}^{(i)}B\left(\overline{x}_i\right){}^{(i)}B^{-1}\left(\overline{x}_{i-1}\right)\left[{}^{(i)}T\left(\overline{x}_{i-1}\right) - {}^{(i)}P\left(\overline{x}_{i-1}\right)\right] + {}^{(i)}P\left(\overline{x}_i\right) \tag{21}
$$

To further extend the relationship presented above, it is necessary to define the interfacial transfer matrix which relates ${}^{(i)}T\left(\overline{x}_{i-1}\right)$ to ${}^{(i-1)}T\left(\overline{x}_{i-1}\right)$. This is done by presenting the continuity conditions in Eq. (9) in terms of vector T defined in Eq. (15):

$$
{}^{(i)}T\left(\overline{x}_{i-1}\right) = {}^{(i-1)}T\left(\overline{x}_{i-1}\right) \tag{22}
$$

Substituting Eq. (22) into (21) gives:

$$
{}^{(i)}T\left(\overline{x}_i\right) = {}^{(i)}B\left(\overline{x}_i\right){}^{(i)}B^{-1}\left(\overline{x}_{i-1}\right)\left[{}^{(i-1)}T\left(\overline{x}_{i-1}\right) - {}^{(i)}P\left(\overline{x}_{i-1}\right)\right] + {}^{(i)}P\left(\overline{x}_i\right) \tag{23}
$$

This relationship relates the vector T of sub-beam i evaluated at its right end to that of sub-beam i-1. Now, the relationship can be further expanded using the local and interfacial transfer matrices of sub-beam i-1 to relate ${}^{(i)}T\left(\overline{x}_i\right)$ to ${}^{(i-2)}T\left(\overline{x}_{i-2}\right)$. Following the same procedure, ${}^{(i)}T\left(\overline{x}_i\right)$ is related to ${}^{(1)}T\left(\overline{x}_0\right)$ as follows:

$$
\begin{aligned}
{}^{(i)}T\left(\bar{x}_i\right) = &\left\{\prod_{k=i}^{1}\left\{{}^{(k)}B\left(\bar{x}_k\right){}^{(k)}B^{-1}\left(\bar{x}_{k-1}\right)\right\}\left\{{}^{(1)}T(\bar{x}_0) - {}^{(1)}P(\bar{x}_0)\right\} + \right. \\
&\left. + \sum_{k=2}^{i}\left(\prod_{j=i}^{k}\left\{{}^{(j)}B(\bar{x}_j){}^{(j)}B^{-1}(\bar{x}_{j-1})\right\}\left\{{}^{(k-1)}P(\bar{x}_{k-1}) - {}^{(k)}P(\bar{x}_{k-1})\right\}\right)\right\} + {}^{(i)}P(\bar{x}_i)
\end{aligned}
\tag{24}
$$

Note that $\prod_{k=i}^{1} F_k = F_i F_{i-1} \ldots F_1$. Eq. (16) is used to express ${}^{(i)}T\left(\bar{x}_i\right)$ and ${}^{(1)}T(\bar{x}_0)$ in Eq. (24), in terms of the vector of the unknown constants. Therefore, the unknown constants of the sub-beam i are related to the unknown constants of the first sub-beam as given below:

$$
\begin{aligned}
{}^{(i)}\begin{bmatrix} A_1 \\ A_2 \\ A_3 \\ A_4 \end{bmatrix} = {}^{(i)}B^{-1}\left(\bar{x}_i\right)&\left\{\prod_{k=i}^{1}\left\{{}^{(k)}B\left(\bar{x}_k\right){}^{(k)}B^{-1}\left(\bar{x}_{k-1}\right)\right\}{}^{(1)}B\left(\bar{x}_0\right) \; {}^{(1)}\begin{bmatrix} A_1 \\ A_2 \\ A_3 \\ A_4 \end{bmatrix} + \right. \\
&\left. + \sum_{k=2}^{i}\left(\prod_{j=i}^{k}\left\{{}^{(j)}B(\bar{x}_j){}^{(j)}B^{-1}(\bar{x}_{j-1})\right\}\left\{{}^{(k-1)}P(\bar{x}_{k-1}) - {}^{(k)}P(\bar{x}_{k-1})\right\}\right)\right\}
\end{aligned}
\tag{25}
$$

for i = 2, …, n. The significance of Eq. (25) lies in its ability to simplify the problem of a nonuniform small-scale beam, containing any arbitrary number of sub-beams, to the task of determining just the four unknown constants of the first sub-beam. These constants can be defined by imposing the boundary conditions presented in Eq. (11). The conditions on the left side of the beam are directly formulated in terms of the unknown constants of the first sub-beam. Also, the conditions on the right side of the beam, which are initially defined in terms of the constants of sub-beam n, are reformulated in terms of the unknown constants of the first sub-beam using Eq. (25) by setting $i = n$. However, this method does not directly lead to the derivation of closed-form solutions. Instead, another approach based on the formulation in [50] is followed in the next section to derive a closed-form solution for the displacement. The notation in the following section is chosen to be similar to that in [50] to highlight the similarities and simplify following the formulation.

3.2. Closed-Form Solutions

The relations in Eqs. (24) and (16) are used to express the vector of unknowns of sub-beam i in terms of ${}^{(1)}T(\bar{x}_0)$:

$$
{}^{(i)}\begin{bmatrix} A_1 \\ A_2 \\ A_3 \\ A_4 \end{bmatrix} = {}^{(i)}B^{-1}\left(\bar{x}_i\right)\left\{\prod_{k=i}^{1}\left\{{}^{(k)}B\left(\bar{x}_k\right){}^{(k)}B^{-1}\left(\bar{x}_{k-1}\right)\right\}\left\{{}^{(1)}T(\bar{x}_0)-{}^{(1)}P(\bar{x}_0)\right\}+\right.
$$

$$
\left.+\sum_{k=2}^{i}\left(\prod_{j=i}^{k}\left\{{}^{(j)}B(\bar{x}_j){}^{(j)}B^{-1}(\bar{x}_{j-1})\right\}\left\{{}^{(k-1)}P(\bar{x}_{k-1})-{}^{(k)}P(\bar{x}_{k-1})\right\}\right)\right\} \tag{26}
$$

Now, the obtained expression for the unknowns of sub-beam i is substituted into Eq. (16) to define ${}^{(i)}T\left(\bar{x}\right)$:

$$
{}^{(i)}T\left(\bar{x}\right) = {}^{(i)}B\left(\bar{x}\right){}^{(i)}B^{-1}\left(\bar{x}_i\right)\left\{\prod_{k=i}^{1}\left\{{}^{(k)}B\left(\bar{x}_k\right){}^{(k)}B^{-1}\left(\bar{x}_{k-1}\right)\right\}\left\{{}^{(1)}T(\bar{x}_0)-{}^{(1)}P(\bar{x}_0)\right\}+\right.
$$

$$
\left.+\sum_{k=2}^{i}\left(\prod_{j=i}^{k}\left\{{}^{(j)}B(\bar{x}_j){}^{(j)}B^{-1}(\bar{x}_{j-1})\right\}\left\{{}^{(k-1)}P(\bar{x}_{k-1})-{}^{(k)}P(\bar{x}_{k-1})\right\}\right)\right\}+{}^{(i)}P\left(\bar{x}\right) \tag{27}
$$

Note that the first element of vector T defined in Eq. (15) is the displacement. Therefore, to define the displacement explicitly, the vector ${}^{(1)}T(\bar{x}_0)$ in Eq. (27) should be derived in closed-form for different boundary conditions.

Fixed-fixed boundary conditions

Considering Eq. (15), the first and second elements of ${}^{(1)}T(\bar{x}_0)$ for a fixed-fixed boundary condition are equal to zero. The third and fourth elements of ${}^{(1)}T(\bar{x}_0)$ are derived using Eqs. (11), (15), and (24) evaluated for $i = n$:

$$
\begin{aligned}
&{}^{(1)}T_1(\bar{x}_0) = 0; \qquad {}^{(1)}T_2(\bar{x}_0) = 0 \\
&{}^{(1)}T_3(\bar{x}_0) = \frac{{}^{(n)}\Omega_{24}}{{}^{(n)}\Omega_{24}\,{}^{(n)}\Omega_{13} - {}^{(n)}\Omega_{14}\,{}^{(n)}\Omega_{23}}\left[\mu_1 - \frac{{}^{(n)}\Omega_{14}}{{}^{(n)}\Omega_{24}}\mu_2\right] \\
&{}^{(1)}T_4(\bar{x}_0) = \frac{\mu_2 - {}^{(n)}\Omega_{23}\,{}^{(1)}T_3(\bar{x}_0)}{{}^{(n)}\Omega_{24}}
\end{aligned} \tag{28}
$$

where μ_k for $k = 1, \ldots, 4$ are:

$$
\mu_k = \sum_{g=1}^{4} {}^{(n)}\Omega_{kg}\;{}^{(1)}P_g(\bar{x}_0) - {}^{(n)}S_k - {}^{(n)}P_k(\bar{x}_n) \tag{29}
$$

and ${}^{(i)}\Omega_{kg}$ and ${}^{(i)}S_k$ are defined by the recursive formulas:

$$
\begin{aligned}
&{}^{(i)}\Omega_{kg} = \sum_{m=1}^{4} {}^{(i)}U_{km}\,{}^{(i-1)}\Omega_{mg} \text{ for } i = 2, ..., n\,;\ {}^{(1)}\Omega_{kg} = {}^{(1)}U_{kg} \\
&{}^{(i)}U_{km} = \sum_{t=1}^{4} {}^{(i)}B_{kt}(\bar{x}_i)\ \ {}^{(i)}B^{-1}{}_{tm}(\bar{x}_{i-1}) \\
&{}^{(i)}S_k = \sum_{q=1}^{4} {}^{(i)}U_{kq}\left[{}^{(i-1)}S_q - {}^{(i)}P_q(\bar{x}_{i-1}) + {}^{(i-1)}P_q(\bar{x}_{i-1})\right] \text{ for } k = 2, ..., n\,;{}^{(1)}S_i = 0
\end{aligned}
\tag{30}
$$

where the elements of ${}^{(i)}B$ and ${}^{(i)}P$ are given in Eqs. (17) and (18).

Fixed-pinned boundary conditions

In this case, the elements of the vector ${}^{(1)}T(\bar{x}_0)$ are:

$$
\begin{aligned}
&{}^{(1)}T_1(\bar{x}_0) = 0; \qquad {}^{(1)}T_2(\bar{x}_0) = 0 \\
&{}^{(1)}T_3(\bar{x}_0) = \frac{{}^{(n)}\Omega_{34}}{{}^{(n)}\Omega_{34}\,{}^{(n)}\Omega_{13} - {}^{(n)}\Omega_{14}\,{}^{(n)}\Omega_{33}}\left[\mu_1 - \frac{{}^{(n)}\Omega_{14}}{{}^{(n)}\Omega_{34}}\mu_3\right] \\
&{}^{(1)}T_4(\bar{x}_0) = \frac{\mu_3 - {}^{(n)}\Omega_{33}\,{}^{(1)}T_3(\bar{x}_0)}{{}^{(n)}\Omega_{34}}
\end{aligned}
\tag{31}
$$

Fixed-free boundary conditions

In this case, the elements of the vector ${}^{(1)}T(\bar{x}_0)$ are:

$$
\begin{aligned}
&{}^{(1)}T_1(\bar{x}_0) = 0; \qquad {}^{(1)}T_2(\bar{x}_0) = 0 \\
&{}^{(1)}T_3(\bar{x}_0) = \frac{{}^{(n)}\Omega_{34}}{{}^{(n)}\Omega_{34}\,{}^{(n)}\Omega_{43} - {}^{(n)}\Omega_{44}\,{}^{(n)}\Omega_{33}}\left[\mu_4 - \frac{{}^{(n)}\Omega_{44}}{{}^{(n)}\Omega_{34}}\mu_3\right] \\
&{}^{(1)}T_4(\bar{x}_0) = \frac{\mu_3 - {}^{(n)}\Omega_{33}\,{}^{(1)}T_3(\bar{x}_0)}{{}^{(n)}\Omega_{34}}
\end{aligned}
\tag{32}
$$

Pinned-pinned boundary conditions

In this case, the elements of the vector ${}^{(1)}T(\bar{x}_0)$ are:

$$
\begin{aligned}
&{}^{(1)}T_1(\bar{x}_0)=0; \qquad {}^{(1)}T_3(\bar{x}_0)=0 \\
&{}^{(1)}T_2(\bar{x}_0)=\frac{{}^{(n)}\Omega_{34}}{{}^{(n)}\Omega_{34}\,{}^{(n)}\Omega_{12}-{}^{(n)}\Omega_{14}\,{}^{(n)}\Omega_{32}}\left[\mu_1-\frac{{}^{(n)}\Omega_{14}}{{}^{(n)}\Omega_{34}}\mu_3\right] \\
&{}^{(1)}T_4(\bar{x}_0)=\frac{\mu_3-{}^{(n)}\Omega_{32}\,{}^{(1)}T_2(\bar{x}_0)}{{}^{(n)}\Omega_{34}}
\end{aligned}
\tag{33}
$$

Having the closed-form solution of the vector ${}^{(1)}T(\bar{x}_0)$ for different boundary conditions given in Eqs. (28), (31), (32), and (33), the displacement of the generic sub-beam i is derived using the first element of the vector ${}^{(i)}T\left(\bar{x}\right)$ defined in Eq. (27):

$$
{}^{(i)}\bar{v}\left(\bar{x}\right)={}^{(i)}P_1(\bar{x})+\sum_{l=1}^{4}\left\{\left[\sum_{r=1}^{4}{}^{(i)}N_{1r}(r)\,{}^{(i)}\Omega_{rl}\right]\left({}^{(1)}T_l(\bar{x}_0)-{}^{(1)}P_l(\bar{x}_0)\right)\right\}+\sum_{t=1}^{4}{}^{(i)}N_{1t}(\bar{x})\,{}^{(i)}S_t \tag{34}
$$

with

$$
{}^{(i)}N_{kr}(r)=\sum_{j=1}^{4}{}^{(i)}B_{kj}(\bar{x})\;\;{}^{(i)}B^{-1}{}_{jr}(\bar{x}_i)\,. \tag{35}
$$

The explicit, closed-form relation provided in Eq. (34) is easily implemented in a computer code and is utilized in the next section to investigate the bending behavior of small-scale beams composed of multiple sub-beams.

4. Numerical Examples and Discussion

The matrix formulation presented in the previous section, particularly the solution given in Eq. (34), facilitates the study of bending behavior in small-scale beams composed of any arbitrary number of sub-beams. Here, the solution is applied to study nonuniform beams with two to five sub-beams.

4.1. Beams with Two Sub-beams

Digrams in Fig. 4 refer to the deflection of a beam made of two sub-beams connected at $\bar{x}_1$. The sub-beams are made of different materials with compliances ${}^{(1)}\bar{C}=2\,{}^{(2)}\bar{C}=1$. Four different boundary conditions are considered and the results are presented for both local and nonlocal ($2\,{}^{(1)}\lambda={}^{(2)}\lambda=0.5$) beams. The case with $\bar{x}_1=0$ refers to a beam made of only the second sub-beam, while $\bar{x}_1=1$ describes a beam made of entirely the first sub-beam.

In local beams and for all the considered boundary conditions, the stiffness of the beam decreases by increasing $\bar{x}_1$. The reason is that by increasing $\bar{x}_1$ from 0 to 1, a larger portion of the beam is made of the first sub-beam which is more compliant compared to the second sub-beam. However, this uniform dependency of the stiffness of the beam on $\bar{x}_1$ does not persist when the nonlocality is considered. In this case, the behavior is more complicated. For instance, the nonlocal cantilever beam with $\bar{x}_1 = 0.1$ is stiffer than the beam made of entirely the second sub-beam, i.e., when $\bar{x}_1 = 0$. This unique behavior, especially pronounced for nonlocal beams with more constrained boundary conditions, is attributed to the non-standard constitutive boundary conditions in Eq. (10) and necessitates experimental investigation.

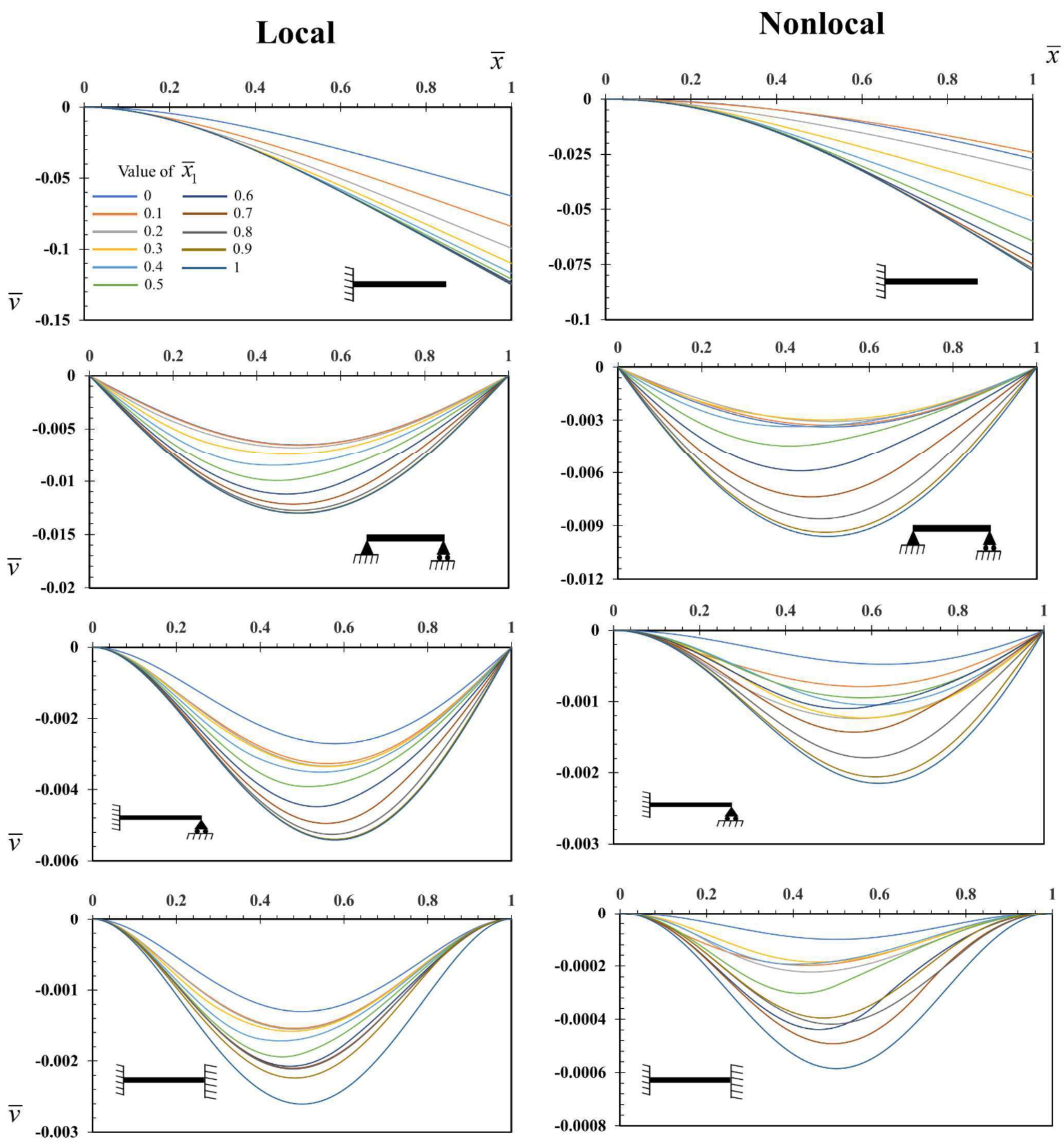

Fig. 4 Deflection of a miniaturized beam with two sub-beams (${}^{(1)}\bar{C} = 2{}^{(2)}\bar{C} = 1$) under a uniform transverse load. Results are presented for local and nonlocal ($2{}^{(1)}\lambda = {}^{(2)}\lambda = 0.5$) beams on varying the location of the cross-section where the sub-beams are connected, $\bar{x}_1$, for different boundary conditions.

The immediate implication of the preceding observation is that dividing a homogeneous miniaturized beam into several sub-beams and subsequently reconnecting them alters the overall stiffness of the beam. This, in turn, offers the opportunity to purposefully design the cutting cross-sections to manipulate the flexural response of the miniaturized beam. This interesting observation is further investigated in Fig. 5. The figure presents the ratio between the deflection of (i) a miniaturized beam composed of two identical sub-beams (${}^{(1)}\bar{C} = {}^{(2)}\bar{C} = 1$ and ${}^{(1)}\lambda = {}^{(2)}\lambda = \lambda$) connected at $\bar{x}_1$, and (ii) the same miniaturized beam composed of only one sub-beam under a uniform transverse load. Results are presented for different nonlocal parameters, fixed-free, and pinned-pinned boundary conditions on varying $\bar{x}_1$. The ratio is given at the free end for the fixed-free beam and at the midspan for the pinned-pinned beam. For the large-scale beam with $\lambda = 0$, dividing it into two sub-beams and reconnecting them yields no difference in the deflection of the beam. This explains why the curves related to the local beam are always equal to one. However, for the small-scale beam with $\lambda \neq 0$, cutting it into two sub-beams and reassembling them increases the stiffness of the miniaturized beam. The impact of cutting and reconnecting the sub-beams on the stiffness of the resulting beam becomes more pronounced for higher values of nonlocal parameters. Interestingly, for any nonlocal parameter, there exists a specific cross-section where the effect of cutting and reconnecting the sub-beams is maximized. The optimal cross-section location for the pinned-pinned beam consistently lies at the mid-span, while it varies with the nonlocal parameter in the fixed-free beam.

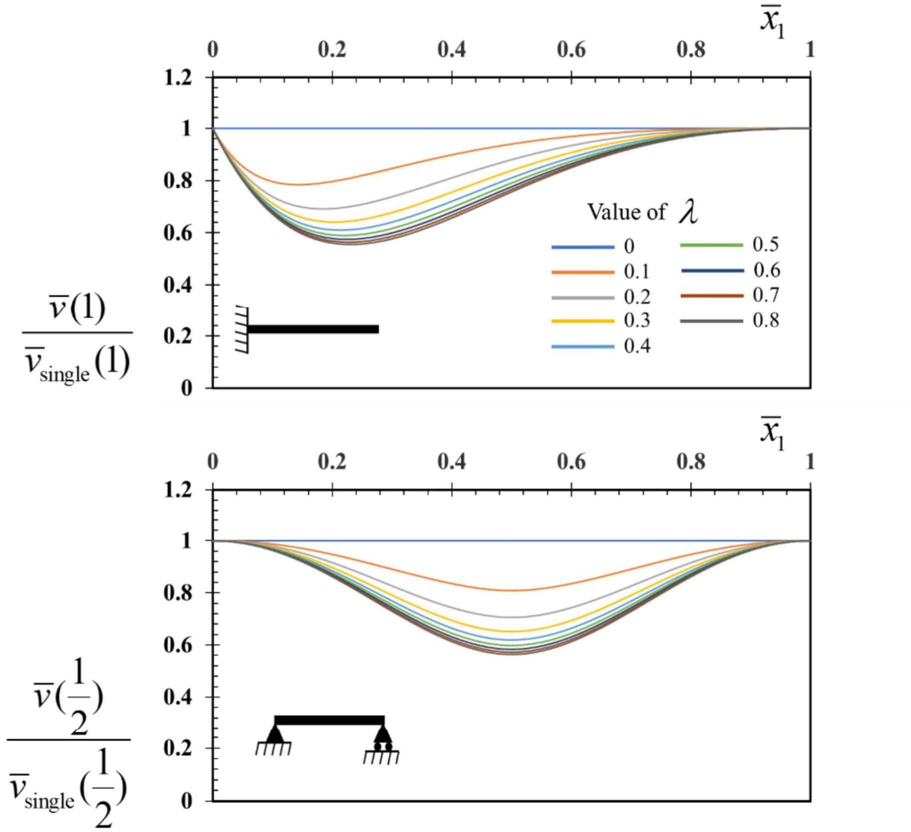

Fig. 5 The ratio between the deflections of a miniaturized beam after, $\bar{v}$, and before, $\bar{v}_{\text{single}}$, cutting and connecting at $\bar{x}_1$ under a uniform transverse load. Results are presented for different nonlocal parameters, fixed-free, and pinned-pinned boundary conditions on varying $\bar{x}_1$.

The effect of the compliance of two sub-beams on the flexural response of miniaturized beams is studied in Fig. 6. Deflection profiles are presented by varying the compliance of the second sub-beam under different boundary conditions. The results refer to the case where the sub-beams are connected at the mid-span and have ${}^{(1)}\bar{C}=1$ and $2\,{}^{(1)}\lambda={}^{(2)}\lambda=0.5$. For all the considered cases, increasing the compliance of the second sub-beam increases the compliance of the beam and its deflection. This behavior is similar to that of the large-scale local beams with two sub-beams. The effect of the second sub-beam's compliance on the deflection of the fixed-free beam is less pronounced than in beams with other boundary conditions, as it experiences lower stress levels being located closer to the free end.

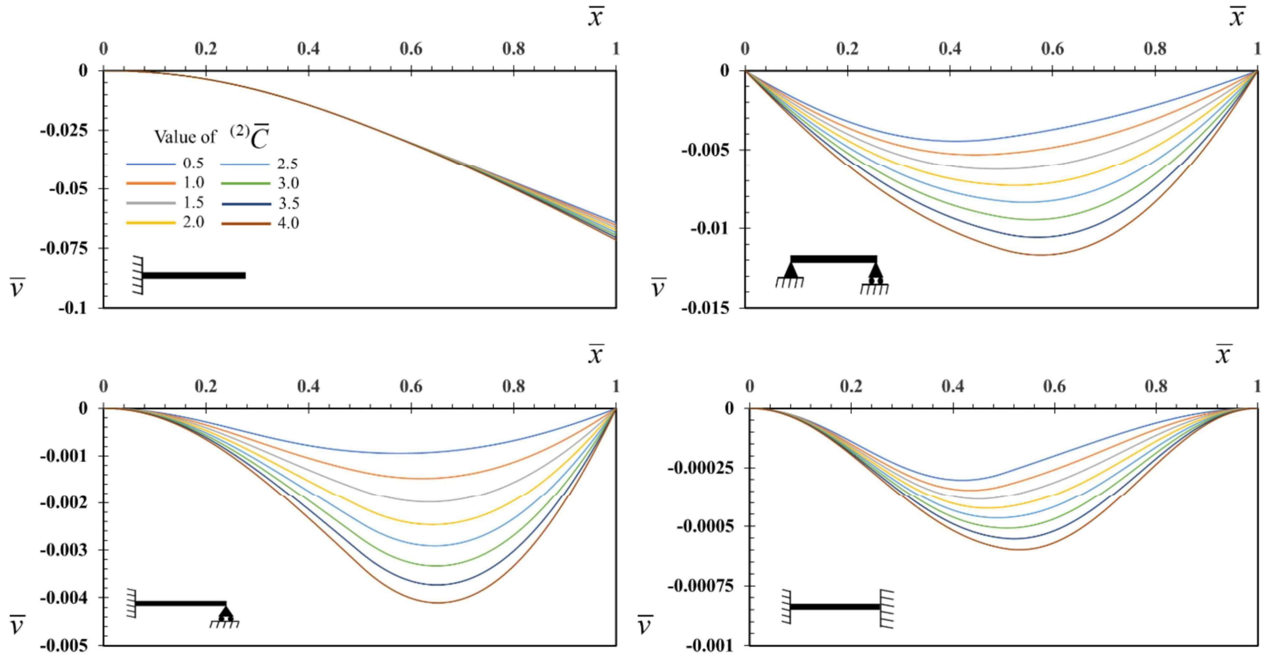

Fig. 6 Deflection of a miniaturized beam with two sub-beams ($^{(1)}\bar{C}=1$ and $2\,^{(1)}\lambda = {}^{(2)}\lambda = 0.5$) under a uniform transverse load. The sub-beams are connected at $\bar{x}_1 = 0.5$ and the results are presented on varying $^{(2)}\bar{C}$ for different boundary conditions.

4.2. Beams with Multiple Sub-beams

The closed-form solution presented in Eq. (34) significantly simplifies the study of the flexural response of nonuniform miniaturized beams with numerous sub-beams. In this section, the relation is applied to investigate the deflection in miniaturized beams composed of three, four, and five sub-beams. Deflections of a beam with three sub-beams having $^{(1)}\bar{C} = {}^{(2)}\bar{C}/2 = 2\,^{(3)}\bar{C} = 1$ and $^{(1)}\lambda = {}^{(2)}\lambda = {}^{(3)}\lambda = 0.25$ under a uniform transverse load are illustrated in Fig. 7. The results are presented for various boundary conditions, varying the location of cross-sections where the sub-beams are connected, i.e., $\bar{x}_1$ and $\bar{x}_2$. Deflections at the free end are shown for the cantilever beam, and at the mid-span for the other beams. For a local nonuniform beam, at a fixed value of $\bar{x}_1$, the deflection increases with an increase in $\bar{x}_2$ (results not shown). This is because an increase in $\bar{x}_2$ elongates the second sub-beam, made of the most compliant material, and shortens the last sub-beam, made of the stiffest material. However, the behavior of the nonlocal nonuniform beam is much more intricate. For instance, in the case where the nonlocal nonuniform beam is fixed at both ends, an increase in $\bar{x}_2$ for a constant value of $\bar{x}_1$ results in an undulating curve.

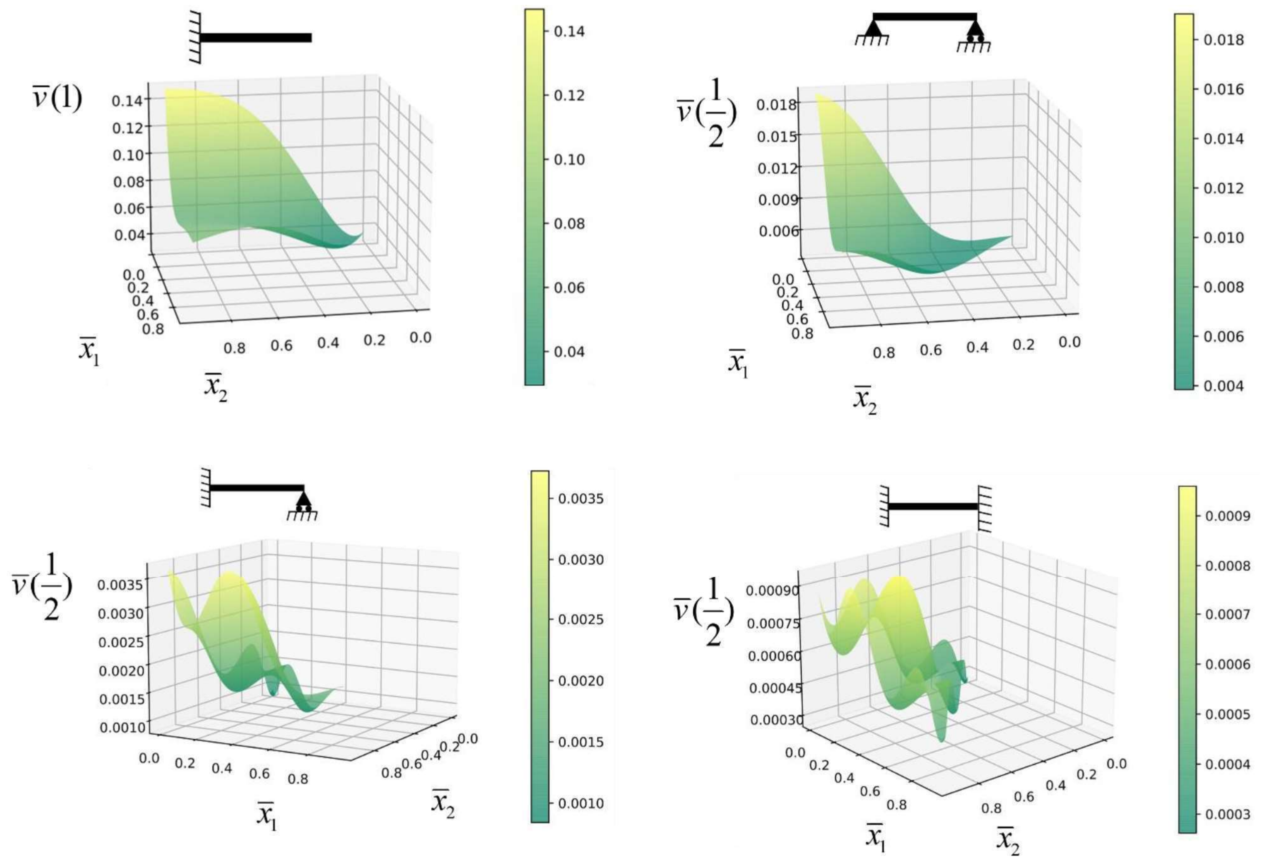

Fig. 7 Deflections of a beam with three sub-beams having ${}^{(1)}\bar{C} = {}^{(2)}\bar{C}/2 = 2\,{}^{(3)}\bar{C} = 1$ and ${}^{(1)}\lambda = {}^{(2)}\lambda = {}^{(3)}\lambda = 0.25$ under a uniform transverse load. The results are presented for different boundary conditions on varying the location of cross-sections where the sub-beams are connected, i.e., $\bar{x}_1$ and $\bar{x}_2$. The deflections are presented at the free end of the cantilever beam and the mid-span of the other beams.

Deflections of a beam with four sub-beams having ${}^{(1)}\bar{C} = {}^{(2)}\bar{C}/2 = {}^{(3)}\bar{C}/3 = {}^{(4)}\bar{C}/4 = 1$ and ${}^{(2)}\lambda = {}^{(3)}\lambda = 0.25$ under a uniform transverse load are depicted in Fig. 8. The sub-beams are connected at fixed locations $\bar{x}_1 = 0.25$, $\bar{x}_2 = 0.5$, and $\bar{x}_3 = 0.75$. The results are presented for different boundary conditions by varying the nonlocal parameters of the first and the fourth sub-beams, i.e., λ_1 and λ_4. Deflections are shown at the free end for the cantilever beam and at the mid-span for the other beams. In all cases, the deflection of the beam decreases for higher values of the nonlocal parameters. The effects of the nonlocal parameters of the first and fourth sub-beams on the deflection are highly dependent on the boundary conditions.

For the cantilever configuration, the impact of the nonlocal parameter of the first sub-beam on the deflection is significantly more pronounced than that of the fourth sub-beam. This is because in a cantilever configuration, the stresses generated in the first sub-beam, closer to the fixed end, are much greater than those generated in the fourth sub-beam, closer to the free end. Based on the same reasoning, the effect of the nonlocal parameter of the fourth sub-beam on the deflection becomes stronger when the right end of the beam is pinned or fixed, i.e., when the boundary condition is fixed-pinned or fixed-fixed. On the other hand, the effect of the nonlocal parameters on the deflection is also influenced by the compliance of the sub-beams. For instance, in a pinned-pinned configuration, the impact of the nonlocal parameter of the fourth sub-beam, which has the highest compliance, on the deflection is more pronounced than the effect of the first sub-beam, which is the stiffest sub-beam.

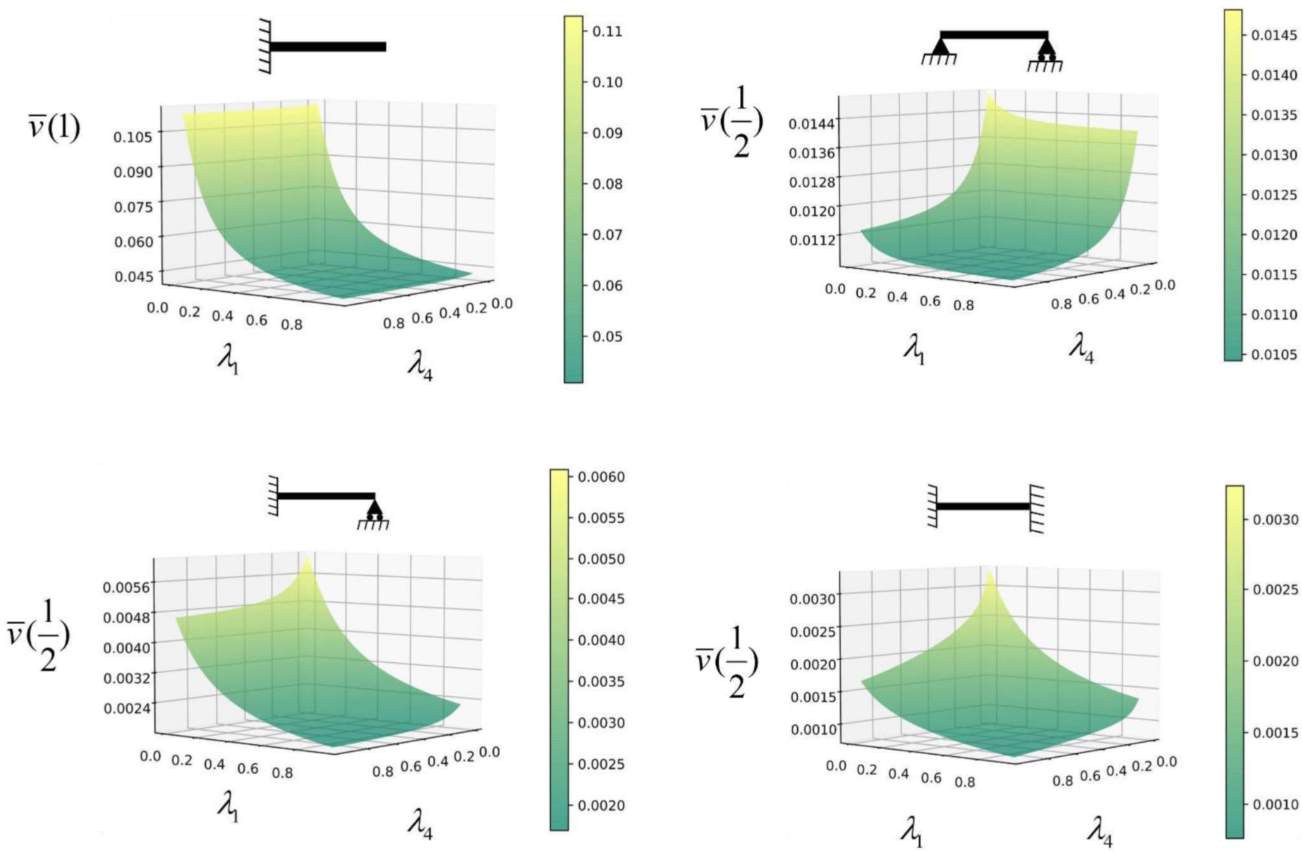

Fig. 8 Deflections of a beam with four sub-beams having ${}^{(1)}\bar{C} = {}^{(2)}\bar{C}/2 = {}^{(3)}\bar{C}/3 = {}^{(4)}\bar{C}/4 = 1$ and ${}^{(2)}\lambda = {}^{(3)}\lambda = 0.25$ under a uniform transverse load. The sub-beams are connected to each other at locations $\bar{x}_1 = 0.25$, $\bar{x}_2 = 0.5$, and $\bar{x}_3 = 0.75$. The results are presented for different boundary conditions on varying the nonlocal parameters of the first and the fourth sub-beams, i.e., λ_1 and λ_4. The deflections are presented at the free end of the cantilever beam and the mid-span of the other beams.

Deflections of a beam with five sub-beams having ${}^{(1)}\bar{C} = {}^{(2)}\bar{C}/4 = {}^{(3)}\bar{C}/5 = {}^{(4)}\bar{C}/3 = {}^{(5)}\bar{C}/2 = 1$ and ${}^{(1)}\lambda = {}^{(2)}\lambda = {}^{(4)}\lambda = {}^{(5)}\lambda = 0.25$ under a uniform transverse load are illustrated in Fig. 9. The sub-beams are connected to each other at locations $\bar{x}_1 = 0.2$, $\bar{x}_3 = 0.6$, and $\bar{x}_4 = 0.8$. The results are presented for different boundary conditions, varying $\bar{x}_2$ and λ_3. Deflections are shown at the free end for the cantilever beam and at the mid-span for the other beams. Increasing $\bar{x}_2$ elongates the second sub-beam and shortens the third sub-beam. In a local nonuniform beam, it is expected that increasing $\bar{x}_2$ reduces the deflection since the second sub-beam is stiffer than the third one. However, data presented in Fig. 9 show that for the nonlocal nonuniform beam, increasing $\bar{x}_2$ may also increase the deflection.

On the other hand, increasing the nonlocal parameter of the third sub-beam consistently reduces the deflection. This is because the stress-driven nonlocal formulation always predicts a stiffening behavior when the nonlocal parameter increases. However, the effect of the nonlocal parameter of the third sub-beam is influenced by the location where the second and third sub-beams are joined. This underscores the inherent flexibility in the design of a nonuniform miniaturized beam to tailor its deflection curve.

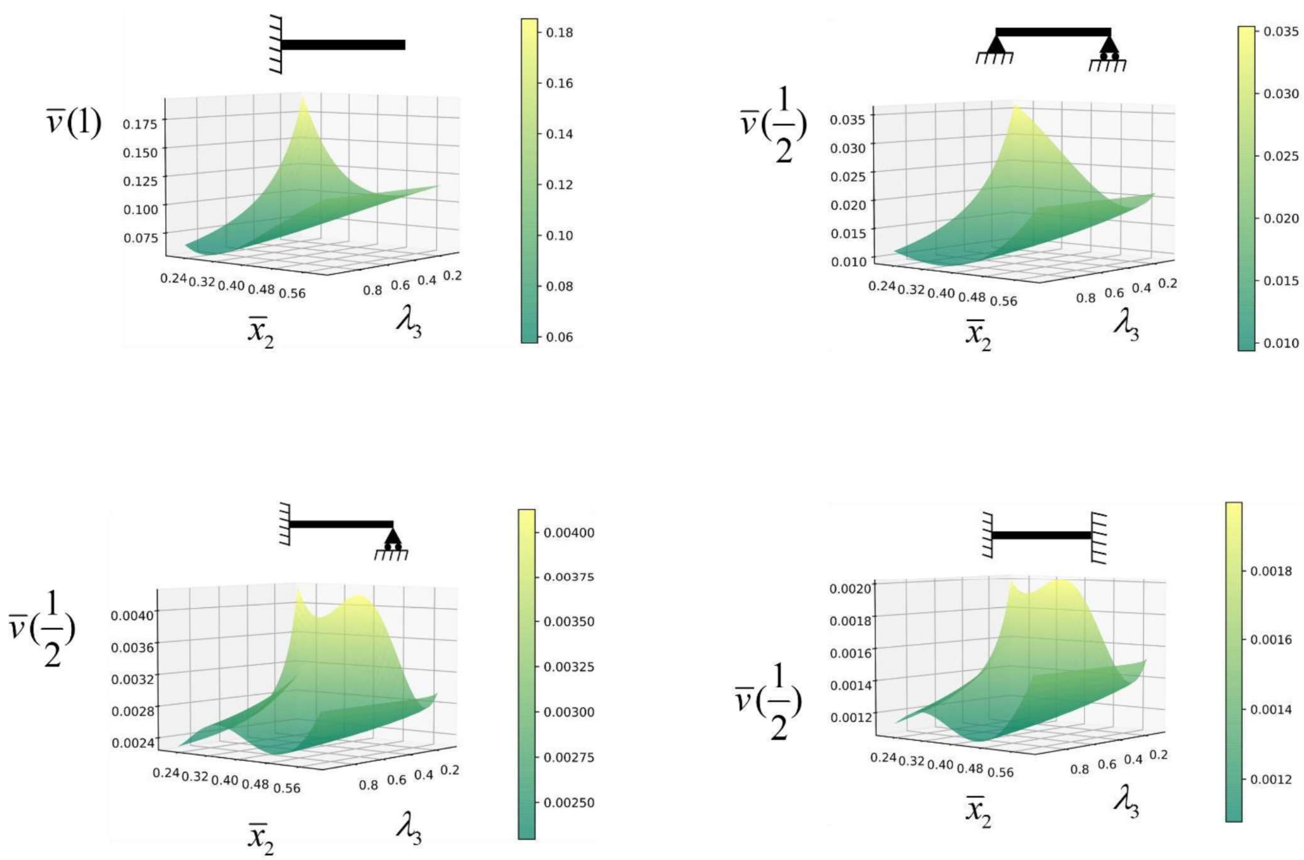

Fig. 9 Deflections of a beam with five sub-beams having ${}^{(1)}\bar{C} = {}^{(2)}\bar{C}/4 = {}^{(3)}\bar{C}/5 = {}^{(4)}\bar{C}/3 = {}^{(5)}\bar{C}/2 = 1$ and ${}^{(1)}\lambda = {}^{(2)}\lambda = {}^{(4)}\lambda = {}^{(5)}\lambda = 0.25$ under a uniform transverse load. The sub-beams are connected to each other at locations $\bar{x}_1 = 0.2$, $\bar{x}_3 = 0.6$, and $\bar{x}_4 = 0.8$. The results are presented for different boundary conditions on

varying $\overline{x}_2$ and λ_3. The deflections are presented at the free end of the cantilever beam and the mid-span of the other beams.

5. Conclusions

A stress-driven nonlocal model has been formulated based on the variational approach and the transfer matrix method to investigate the flexural response of nonuniform miniaturized beams made of different sub-beams with different material and geometrical properties. The model expresses the curvature at any position within a sub-beam through an integral convolution involving the bending moments exclusively across that sub-beam and a kernel function. The validity of the model relies on the assumption of independent nonlocalities among sub-beams. Solving the equilibrium equations governing the bending deflection of individual sub-beams under uniform loading, we obtained explicit closed-form solutions in terms of some unknown constants. Utilizing the transfer matrix method, we defined these constants, presenting explicit solutions for the deflections of nonuniform beams with any arbitrary number of sub-beams. Applying these closed-form solutions, we explored nonuniform miniaturized beams featuring two to five sub-beams. The results emphasize the intricate flexural response of nonlocal nonuniform beams, revealing their complexity in contrast to the more predictable behavior observed in the bending of local nonuniform beams. Specifically, in local nonuniform beams, increasing the length of a stiff sub-beam increases the overall system stiffness. However, in nonlocal nonuniform beams, this behavior is unpredictable, and in some instances, elongating the stiff sub-beam may lead to a more compliant overall response. The phenomenon is influenced by the type of boundary conditions. The implication of this observation, which may be of importance in the Engineering Science community, is that dividing a uniform miniaturized beam into multiple sub-beams and then reconnecting them alters the overall stiffness of the beam. Upon experimental validation, the presented results open the possibility of intentionally designing cutting cross-sections to engineer the flexural response of the miniaturized beam.

Funding

The author gratefully acknowledges the financial support provided by the National Science Centre (NCN) in Poland through the grant agreement No: UMO-2022/47/D/ST8/01348.

Statements and Declarations

The authors declare that they have no known competing financial interests or personal relationships that could have appeared to influence the work reported in this paper.

References

1. Roukes, M. (2001). Nanoelectromechanical systems face the future. *Physics World*, *14*(2), 25. https://doi.org/10.1088/2058-7058/14/2/29
2. Kalinin, S. V., Karapetian, E., & Kachanov, M. (2004). Nanoelectromechanics of piezoresponse force microscopy. *Physical Review B*, *70*(18), 184101. https://doi.org/10.1103/PhysRevB.70.184101
3. Kalinin, S. V., Gruverman, A., Rodriguez, B. J., Shin, J., Baddorf, A. P., Karapetian, E., & Kachanov, M. (2005). Nanoelectromechanics of polarization switching in piezoresponse force microscopy. *Journal of Applied Physics*, *97*(7), 074305. https://doi.org/10.1063/1.1866483
4. Karapetian, E., Kachanov, M., & Kalinin, S. V. (2005). Nanoelectromechanics of piezoelectric indentation and applications to scanning probe microscopies of ferroelectric materials. *Philosophical Magazine*, *85*(10), 1017–1051. https://doi.org/10.1080/14786430412331324680
5. Ghayesh, M. H., Farokhi, H., & Gholipour, A. (2017). Oscillations of functionally graded microbeams. *International Journal of Engineering Science*, *110*, 35–53. https://doi.org/10.1016/j.ijengsci.2016.09.011
6. Yee, K., & Ghayesh, M. H. (2023). A review on the mechanics of graphene nanoplatelets reinforced structures. *International Journal of Engineering Science*, *186*, 103831. https://doi.org/10.1016/j.ijengsci.2023.103831
7. Ghayesh, M. H., & Farajpour, A. (2019). A review on the mechanics of functionally graded nanoscale and microscale structures. *International Journal of Engineering Science*, *137*, 8–36. https://doi.org/10.1016/j.ijengsci.2018.12.001
8. Civalek, Ö., Uzun, B., & Yaylı, M. Ö. (2023). On nonlinear stability analysis of saturated embedded porous nanobeams. *International Journal of Engineering Science*, *190*, 103898. https://doi.org/10.1016/j.ijengsci.2023.103898
9. Wang, S., Ding, W., Li, Z., Xu, B., Zhai, C., Kang, W., … Li, Y. (2023). A size-dependent quasi-3D model for bending and buckling of porous functionally graded curved nanobeam. *International Journal of Engineering Science*, *193*, 103962. https://doi.org/10.1016/j.ijengsci.2023.103962
10. Xu, X., Karami, B., & Shahsavari, D. (2021). Time-dependent behavior of porous curved nanobeam. *International Journal of Engineering Science*, *160*, 103455. https://doi.org/10.1016/j.ijengsci.2021.103455
11. Karami, B., & Ghayesh, M. H. (2023). Vibration characteristics of sandwich microshells with porous functionally graded face sheets. *International Journal of Engineering Science*, *189*, 103884. https://doi.org/10.1016/j.ijengsci.2023.103884
12. Milić, D., Deng, J., Stojanović, V., & Petković, M. D. (2024). Dynamic stability of the sandwich nano-beam system. *International Journal of Engineering Science*, *194*, 103973. https://doi.org/10.1016/j.ijengsci.2023.103973
13. Vattré, A., & Pan, E. (2021). Thermoelasticity of multilayered plates with imperfect interfaces. *International Journal of Engineering Science*, *158*, 103409. https://doi.org/10.1016/j.ijengsci.2020.103409
14. Barretta, R., Čanađija, M., & Marotti de Sciarra, F. (2020). On thermomechanics of multilayered beams. *International Journal of Engineering Science*, *155*, 103364. https://doi.org/10.1016/j.ijengsci.2020.103364
15. Kushch, V. I. (2023). Atomistic and continuum modeling of nanoparticles: Elastic fields, surface constants, and effective stiffness. *International Journal of Engineering Science*, *183*, 103806. https://doi.org/10.1016/j.ijengsci.2022.103806
16. Shariati, M., Azizi, B., Hosseini, M., & Shishesaz, M. (2021). On the calibration of size parameters related to non-classical continuum theories using molecular dynamics simulations. *International Journal of Engineering Science*, *168*, 103544. https://doi.org/10.1016/j.ijengsci.2021.103544
17. Mindlin, R. D., & Tiersten, H. F. (1962). Effects of couple-stresses in linear elasticity. *Archive for Rational Mechanics and Analysis*, *11*(1), 415–448. https://doi.org/10.1007/BF00253946

18. Mindlin, R. D. (1964). Micro-structure in linear elasticity. *Archive for Rational Mechanics and Analysis*, *16*(1), 51–78. https://doi.org/10.1007/BF00248490
19. Eringen, A. C. (1966). Linear Theory of Micropolar Elasticity. *Journal of Mathematics and Mechanics*, *15*(6), 909–923.
20. Eringen, A. C., & Edelen, D. G. B. (1972). On nonlocal elasticity. *International Journal of Engineering Science*, *10*(3), 233–248. https://doi.org/10.1016/0020-7225(72)90039-0
21. Gurtin, M. E., & Ian Murdoch, A. (1975). A continuum theory of elastic material surfaces. *Archive for Rational Mechanics and Analysis*, *57*(4), 291–323. https://doi.org/10.1007/BF00261375
22. Carpinteri, A. (1994). Fractal nature of material microstructure and size effects on apparent mechanical properties. *Mechanics of Materials*, *18*(2), 89–101. https://doi.org/10.1016/0167-6636(94)00008-5
23. Yang, F., Chong, A. C. M., Lam, D. C. C., & Tong, P. (2002). Couple stress based strain gradient theory for elasticity. *International Journal of Solids and Structures*, *39*(10), 2731–2743. https://doi.org/10.1016/S0020-7683(02)00152-X
24. Lam, D. C. C., Yang, F., Chong, A. C. M., Wang, J., & Tong, P. (2003). Experiments and theory in strain gradient elasticity. *Journal of the Mechanics and Physics of Solids*, *51*(8), 1477–1508. https://doi.org/10.1016/S0022-5096(03)00053-X
25. Lim, C. W., Zhang, G., & Reddy, J. N. (2015). A higher-order nonlocal elasticity and strain gradient theory and its applications in wave propagation. *Journal of the Mechanics and Physics of Solids*, *78*, 298–313. https://doi.org/10.1016/j.jmps.2015.02.001
26. Jiang, Y., Li, L., & Hu, Y. (2023). Strain gradient viscoelasticity theory of polymer networks. *International Journal of Engineering Science*, *192*, 103937. https://doi.org/10.1016/j.ijengsci.2023.103937
27. Darban, H., Luciano, R., Caporale, A., & Fabbrocino, F. (2020). Higher modes of buckling in shear deformable nanobeams. *International Journal of Engineering Science*, *154*, 103338. https://doi.org/10.1016/j.ijengsci.2020.103338
28. Attia, M. A. (2017). On the mechanics of functionally graded nanobeams with the account of surface elasticity. *International Journal of Engineering Science*, *115*, 73–101. https://doi.org/10.1016/j.ijengsci.2017.03.011
29. Jin, Q., & Ren, Y. (2024). Review on mechanics of fluid-conveying nanotubes. *International Journal of Engineering Science*, *195*, 104007. https://doi.org/10.1016/j.ijengsci.2023.104007
30. Ahmadi Arpanahi, R., Eskandari, A., Mohammadi, B., & Hosseini Hashemi, S. (2023). Study on the effect of viscosity and fluid flow on buckling behavior of nanoplate with surface energy. *Results in Engineering*, *18*, 101078. https://doi.org/10.1016/j.rineng.2023.101078
31. Faghidian, S. A. (2020). Higher–order nonlocal gradient elasticity: A consistent variational theory. *International Journal of Engineering Science*, *154*, 103337. https://doi.org/10.1016/j.ijengsci.2020.103337
32. Darban, H. (2023). Size effect in ultrasensitive micro- and nanomechanical mass sensors. *Mechanical Systems and Signal Processing*, *200*, 110576. https://doi.org/10.1016/j.ymssp.2023.110576
33. Darban, H., Fabbrocino, F., & Luciano, R. (2020). Size-dependent linear elastic fracture of nanobeams. *International Journal of Engineering Science*, *157*, 103381. https://doi.org/10.1016/j.ijengsci.2020.103381
34. Li, P., Li, W., Tan, Y., Fan, H., & Wang, Q. (2024). A phase field fracture model for ultra-thin micro-/nano-films with surface effects. *International Journal of Engineering Science*, *195*, 104004. https://doi.org/10.1016/j.ijengsci.2023.104004
35. Faghidian, S. A., Żur, K. K., & Pan, E. (2023). Stationary variational principle of mixture unified gradient elasticity. *International Journal of Engineering Science*, *182*, 103786. https://doi.org/10.1016/j.ijengsci.2022.103786

36. Yang, W., Wang, S., Kang, W., Yu, T., & Li, Y. (2023). A unified high-order model for size-dependent vibration of nanobeam based on nonlocal strain/stress gradient elasticity with surface effect. *International Journal of Engineering Science*, *182*, 103785. https://doi.org/10.1016/j.ijengsci.2022.103785
37. Ahmadi Arpanahi, R., Mohammadi, B., Ahmadian, M. T., & Hashemi, S. H. (2023). Study on the buckling behavior of nonlocal nanoplate submerged in viscous moving fluid. *International Journal of Dynamics and Control*, *11*(6), 2820–2830. https://doi.org/10.1007/s40435-023-01166-w
38. Darban, H., Luciano, R., & Basista, M. (2022). Free transverse vibrations of nanobeams with multiple cracks. *International Journal of Engineering Science*, *177*, 103703. https://doi.org/10.1016/j.ijengsci.2022.103703
39. Faghidian, S. A., Żur, K. K., & Reddy, J. N. (2022). A mixed variational framework for higher-order unified gradient elasticity. *International Journal of Engineering Science*, *170*, 103603. https://doi.org/10.1016/j.ijengsci.2021.103603
40. Numanoğlu, H. M., & Civalek, Ö. (2024). On shear-dependent vibration of nano frames. *International Journal of Engineering Science*, *195*, 103992. https://doi.org/10.1016/j.ijengsci.2023.103992
41. Caporale, A., Darban, H., & Luciano, R. (2022). Nonlocal strain and stress gradient elasticity of Timoshenko nano-beams with loading discontinuities. *International Journal of Engineering Science*, *173*, 103620. https://doi.org/10.1016/j.ijengsci.2021.103620
42. Mikhasev, G., Radi, E., & Misnik, V. (2024). Modeling pull-in instability of CNT nanotweezers under electrostatic and van der Waals attractions based on the nonlocal theory of elasticity. *International Journal of Engineering Science*, *195*, 104012. https://doi.org/10.1016/j.ijengsci.2023.104012
43. Ahmadi Arpanahi, R. A., Hashemi, K. H., Mohammadi, B., & Hashemi, S. H. (2023). Investigation of the vibration behavior of nano piezoelectric rod using surface effects and non-local elasticity theory. *Engineering Research Express*, *5*(3), 035029. https://doi.org/10.1088/2631-8695/aced37
44. Darban, H., Caporale, A., & Luciano, R. (2021). Nonlocal layerwise formulation for bending of multilayered/functionally graded nanobeams featuring weak bonding. *European Journal of Mechanics - A/Solids*, *86*, 104193. https://doi.org/10.1016/j.euromechsol.2020.104193
45. Liebold, C., & Müller, W. H. (2016). Comparison of gradient elasticity models for the bending of micromaterials. *Computational Materials Science*, *116*, 52–61. https://doi.org/10.1016/j.commatsci.2015.10.031
46. Tang, C., & Alici, G. (2011). Evaluation of length-scale effects for mechanical behaviour of micro- and nanocantilevers: II. Experimental verification of deflection models using atomic force microscopy. *Journal of Physics D: Applied Physics*, *44*(33), 335502. https://doi.org/10.1088/0022-3727/44/33/335502
47. Romano, G., & Barretta, R. (2017). Nonlocal elasticity in nanobeams: the stress-driven integral model. *International Journal of Engineering Science*, *115*, 14–27. https://doi.org/10.1016/j.ijengsci.2017.03.002
48. Thomson, W. T. (1950). Transmission of Elastic Waves through a Stratified Solid Medium. *Journal of Applied Physics*, *21*(2), 89–93. https://doi.org/10.1063/1.1699629
49. Haskell, A. N. (1953). The dispersion of surface waves in multi-layered media. *Bulletin of the Seismological Society of America*, *43*, 17–34.
50. Darban, H., & Massabò, R. (2018). Thermo-elastic solutions for multilayered wide plates and beams with interfacial imperfections through the transfer matrix method. *Meccanica*, *53*(3), 553–571. https://doi.org/10.1007/s11012-017-0657-6